Appl. Phys. A 69, 597–603 (1999) / Digital Object Identifier (DOI) 10.1007/s003399900166

Applied Physics A
Materials
Science & Processing
© Springer-Verlag 1999

Invited paper

The critical thickness of silicon-germanium layers grown by liquid phase epitaxy

T. Füller[1], M. Konuma[2], J. Zipprich[1], F. Banhart[1,*]

[1] Max-Planck-Institut für Metallforschung, Heisenbergstr. 1, D-70569 Stuttgart, Germany
[2] Max-Planck-Institut für Festkörperforschung, Heisenbergstr. 1, D-70569 Stuttgart, Germany

Received: 29 July 1999/Accepted: 29 July 1999/Published online: 27 October 1999

Abstract. Silicon-germanium layers are grown from metallic solution on (100) and (111) silicon substrates. On (111) Si, coherently strained dislocation-free SiGe layers are obtained with thicknesses larger than predicted by the current models of misfit-induced strain relaxation. A comprehensive characterisation by imaging, diffraction, and analytical electron microscopy techniques is carried out to determine the critical thickness, study the onset of plastic relaxation, and explain the particular growth mechanisms leading to an unexpectedly high thickness of elastically strained SiGe layers. A vertical Ge concentration gradient and the formation of step edges on the layers, where lateral strain relaxes locally, explain the high critical thickness. The model of Matthews and Blakeslee is modified in order to match the experimental observations for solution-grown SiGe layers.

PACS: 61.16.Bg; 61.72.Cc; 81.15.Lm

Heteroepitaxial Ge or SiGe layers on Si substrates are of interest for basic research as well as for device applications [1]. For devices of high performance, a very low density of crystallographic defects such as dislocations is substantial. The main problem of SiGe epitaxy on Si is the lattice mismatch f of up to 4.2% between the Si substrate and the SiGe layer. Pseudomorphic, i.e., dislocation-free growth of a strained layer is only feasible up to a critical thickness h_c of the layer. When the layer thickness exceeds h_c, strain relaxes by the formation of misfit dislocations. The basic theoretical concepts for the understanding of the critical thickness are (a) the model of Ball and Van der Merwe [2], which is based on the minimisation of the sum of the elastic energy in the strained system and the energy introduced by misfit dislocations, (b) the model of Matthews and Blakeslee [3], which considers the forces influencing already existing threading dislocations and their glide, (c) the model of Matthews [4, 5], which assumes the nucleation of dislocation loops and their spreading from the surface to the interface.

* Corresponding author. (Fax: +49-711/689-1010, E-mail: banhart@wselix.mpi-stuttgart.mpg.de)

Some experimentally derived values for h_c of SiGe on Si grown by molecular beam epitaxy (MBE) or chemical vapour deposition (CVD) were larger than predicted by theory [6]. Accordingly, the models have been modified to reproduce the experimentally obtained critical thickness of MBE- or CVD-grown SiGe layers [6, 7].

Liquid phase epitaxy (LPE) of SiGe and Ge on Si(111) substrates has not only shown to yield layers in exceptional crystallographic and electronic quality [8]; the layers have also a higher critical thickness than predicted by the above-stated models. A critical thickness of 4 nm has been reported for a layer with 85 at. % Ge [9]. On (100) substrates, however, LPE SiGe and Ge layers grow always in a Stranski–Krastanov mode [10] where the wetting layer is thinner than h_c. The reasons for the large h_c of LPE SiGe layers on (111) Si have been suspected to be the proximity of thermodynamic equilibrium and the energetic and geometric advantage of the (111) interface. However, a detailed explanation has not been presented until now. The discrepancy between the theoretical predictions and the experimental achievements is of considerable importance. On the one hand, this discrepancy challenges the current understanding of the mechanisms of strain relaxation; on the other hand, a possible new route towards the production of SiGe layers of hitherto unattained quality comes into sight.

The goal of the present study is to solve this discrepancy between the experimentally observed h_c and the calculated predictions of different models [11]. For this purpose, the growth mechanisms of pseudomorphic layers with different Ge contents on Si(111) substrates, with main emphasis on concentrations around 50 at. %, are studied in detail. The particular Ge content of 50% is useful for obtaining pseudomorphic SiGe layers with a thickness of 10 nm or even more, which allows a detailed electron microscopy investigation. Furthermore, Ge-rich layers on Si(100) substrates are grown and characterised.

In this work, a variety of electron microscopy techniques are used for a comprehensive characterisation of SiGe layers. Imaging, diffraction, and analytical techniques are combined and applied to specific problems. For the first time, the analysis of rocking profiles in convergent beam electron diffraction

patterns is applied to obtain unknown material parameters. The entirety of these techniques allows us to carry out a precise measurement of the critical thickness and the composition as well as a detailed analysis of strain fields and strain-induced defects.

1 Experimental

In liquid phase epitaxy of semiconductors, crystallisation occurs from a metallic solution close to thermodynamic equilibrium [12]. The quality of the surface of the substrates prior to growth, in particular the absence of oxide, is of paramount importance. The Si substrates in this work were initially cleaned by an RCA treatment [13], followed by a (2.5%) HF dip and an in situ oxide desorption at 920 °C under hydrogen atmosphere. $Si_{1-x}Ge_x$ layers were grown with various compositions between $0.25 < x < 0.8$ on Si(100) and Si(111) substrates. The lattice mismatch of these systems ranges between 1% and 3.4%. The substrates had a deliberate miscut of $0.2° \pm 0.1°$; the miscut was aligned in $[11\bar{2}]$ on (111) substrates and in [001] on (100) substrates.

The growth experiments were carried out in a facility with a tilt-slide crucible which had the advantage that both the saturation of the solvent and the growth procedure could be carried out without the necessity of opening the reactor tube and exposing the material to air. The growth temperatures ranged between 880 °C and 920 °C. For these experiments, bismuth was chosen as solvent because the solubility of Si in Bi is low and therefore allows control of the growth with almost monolayer precision. Furthermore, the unintentional dissolution of the substrate is reduced to a minimum.

The SiGe layers on Si(100) were grown by applying interfacial energy epitaxy (IEE), a technique which has been introduced by Hansson et al. [14]. The concept of this LPE technique is to reduce the driving force for the crystallisation by choosing a growth temperature lower than the saturation temperature; the solution is therefore undersaturated during growth. Here, growth is solely promoted by the gain in interfacial energy. The temperature difference between growth and saturation was here about 100 °C. The contact time between solution and substrate was varied between 5 s and 120 s.

To obtain pseudomorphic SiGe layers on Si(111) substrates, a growth temperature very close to the saturation temperature was chosen. The contact time between substrate and solution had to be less than 1 s. This exceptionally short growth time is necessary because a large vertical growth rate of up to 250 nm/s begins as soon as h_c is exceeded.

The characterisation of the epitaxial layers was carried out by transmission electron microscopy (TEM) with various imaging, diffraction, and analytical techniques such as bright- and dark-field or lattice imaging, energy dispersive X-ray analysis (EDX), and convergent beam electron diffraction (CBED). Within this work, the analysis of rocking profiles in energy-filtered CBED patterns [15] has been applied for the first time in a routine characterisation study. Furthermore, the growth results were characterised by optical microscopy, scanning electron microscopy (SEM), and atomic force microscopy (AFM).

2 Results

2.1 SiGe *layers on* Si(100) *substrates*

Prior to growth experiments, the influence of the initial thermal treatment of the substrate in hydrogen atmosphere on the arrangement of surface steps was studied. The morphology of (100) surfaces, in particular the arrangement and height of monoatomic surface steps, showed to be unaltered by the annealing, in contrast to (111) substrates (see below).

The growth of flat (two-dimensional) pseudomorphic SiGe layers with large thickness on Si(100) turned out to be impossible by LPE because the growth follows always a Stranski–Krastanov mode with the formation of islands on a thin wetting layer. The thickness of the 2D wetting layer is always smaller than h_c. Figure 1 shows a cross-sectional bright-field TEM image of a SiGe layer on (100) Si. Even in the islands, no misfit- or threading dislocations appear. Strain relaxation seems therefore to occur solely by the formation of islands. Distinct strain contrasts in the substrate region beneath the SiGe islands are visible. Between the islands the thin wetting layer appears as a dark line. The islands in that initial state of growth (after a few seconds growth time) have a base length of 200 nm and a height of 75 nm. The vertical growth rate is higher than 50 nm/s. The islands with the typical shape of pyramids are terminated by (111) facets. EDX measurements show an increase of the Ge concentration with increasing height of the islands.

The approximate thickness of the wetting layer can be determined by HRTEM. Figure 2 shows a lattice image of the SiGe wetting layer. Because of the strain in layer and substrate and a gradient in the Ge concentration, the localisation of the interface between layer and substrate is more difficult than in systems with abrupt concentration changes [16]. A thickness of 8 ± 4 monolayers is determined with a Ge content of 50 at. % in the layer.

2.2 SiGe *layers on* Si(111) *substrates*

The (111) substrates show drastic alterations during the initial tempering. During this process the solvent (here, Bi) is

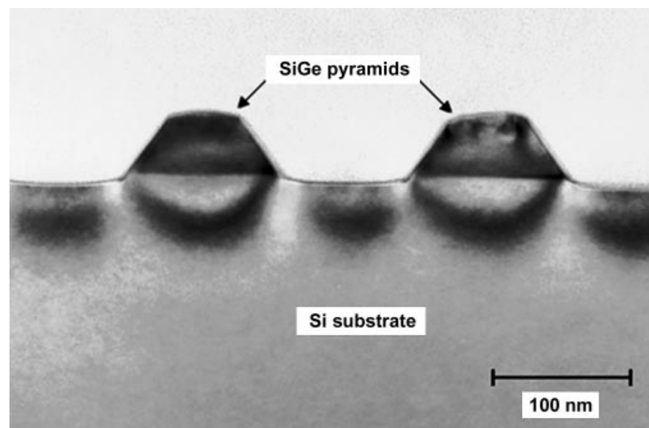

Fig. 1. Cross-sectional TEM image of a SiGe structure grown on a (100) Si substrate. The pyramidal islands are dislocation-free but induce large strains in the substrate as seen from the bend contours. The average Ge concentration in the islands is approximately 50%

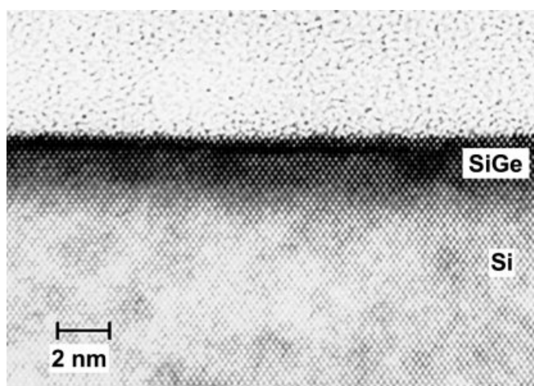

Fig. 2. Lattice-resolution TEM image of a $Si_{0.5}Ge_{0.5}$ wetting layer on a (100) Si substrate. The substrate–layer interface can not be precisely localised due to a Ge concentration gradient and lattice strains. The layer thickness is roughly 8 monolayers

present in the growth chamber but not in contact with the substrate. The hydrogen together with the vapour of the solvent lead to a modification of the (111) surface. Steps of initially monoatomic height accumulate and form macrosteps with a height of 1–4 nm and an interdistance of approximately 1 µm. The AFM image of a tempered Si(111) surface is shown in Fig. 3. The direction of the step edges is solely determined by the misorientation of the substrate. The height and interdistance of the steps increase with increasing temperature and duration of the treatment. Step bunching can not be detected without any metallic solvent in the growth chamber.

The (111) substrate surface proves to be superior to (100) for the growth of 2D layers in an equilibrium process. The best results are achieved with a precisely saturated solution at equilibrium temperature and extremely short contact times between solution and substrate. The growth intervals here are shorter than 1 s. The presence of substrate surface steps has a strong influence on the surface morphology of the layers. As can be seen in the NDIC micrograph in Fig. 4, the layer surface is stepped; the average step height is 10 nm. Since the layer between the steps grows always with a perfect (111) surface and the substrate has a misorientation off the (111) direction, the layer exhibits a sawtooth profile as shown schematically in Fig. 5. After growth periods longer than ∼ 1 s, trapezoidal islands appear on the wetting layer (as seen in Fig. 4). These islands are terminated by perfect (111) top facets; they grow with a vertical rate of more than 250 nm/s.

The stepped layer is almost defect-free when the contact time between solution and substrate is less than 1 s (Figs. 6 and 8). However, at the interface between the large trapezoidal islands and the substrate a misfit dislocation network appears. Figure 6 shows a cross-sectional lattice-resolution image of a step in a pseudomorphic layer. Here, the interface is not visible although Ge is clearly detectable in the layer by EDX. (The localisation of the interface is facilitated, how-

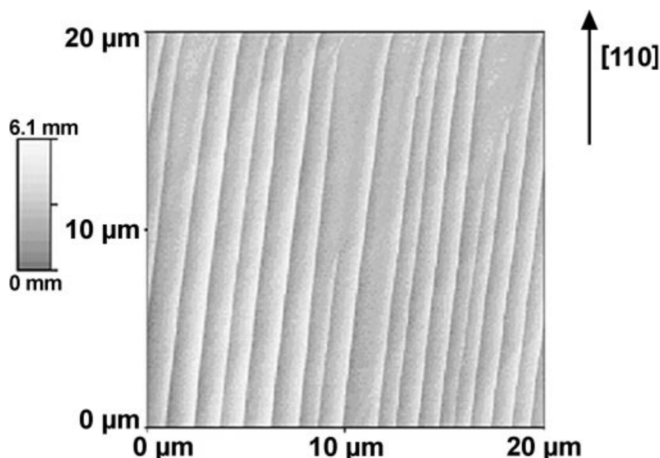

Fig. 3. AFM image showing the surface of a (111) Si substrate after tempering at 920 °C for 4 h. Bunching of monoatomic steps has led to macroscopic steps with heights of 1–4 nm

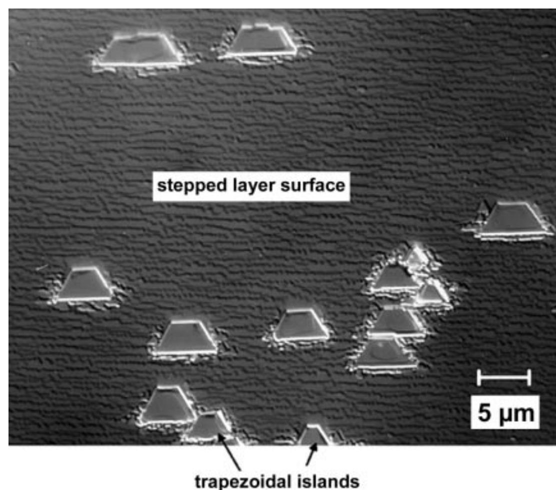

Fig. 4. Optical NDIC micrograph from the surface of a SiGe layer on a (111) Si substrate. The coherent defect-free wetting layer shows steps of 5–10 nm in height. Trapezoidal islands have a larger thickness and contain dislocations

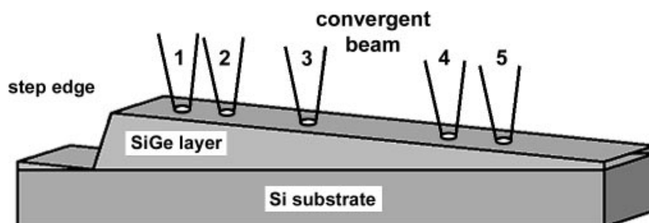

Fig. 5. Schematic drawing of the wedge-shaped profile of a stepped SiGe layer grown on (111) Si. The positions of the convergent electron probe are specified in Table 1

Table 1. Results from the analysis of rocking profiles in convergent beam electron diffraction patterns. Thickness and Ge concentration were measured at several positions of a wedge-shaped SiGe layer on (111) Si. The positions of the electron probe are shown schematically in Fig. 5

Position	Distance from step edge/µm	Layer thickness /nm	Average Ge concentration/%
1	0.1	23.9 ± 0.5	13
2	0.2	22.9	11
3	0.4	17.4	10
4	0.7	8.7	∼ 7
5	0.8	4.9	∼ 7

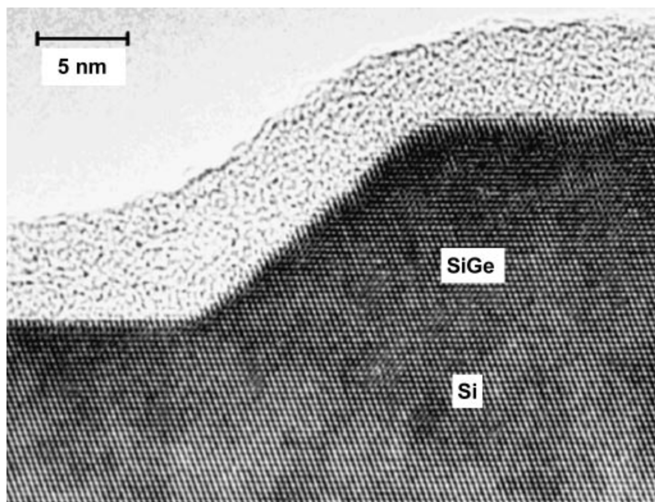

Fig. 6. Lattice-resolution TEM image showing the cross section of a step edge in a SiGe layer grown on (111) Si. The substrate–layer interface does not show up here due to a vertical Ge concentration gradient in the layer

ever, when misfit dislocations are present.) The reason for the lack of contrast features at the interface is a Ge gradient in the layer. The measurement of the Ge concentration profile by EDX on a cross-sectional TEM specimen is shown in Fig. 7. The measurements were carried out in a dedicated STEM with an electron probe of 1 nm in diameter. No sharp chemical interface between the Si substrate and the SiGe layer exists. A vertical gradient of the Ge concentration prevails within approximately 15 nm from the interface. Therefore, the nominal Ge concentration is reached only at a greater distance from the interface. Accordingly, the average Ge concentration in the layer is lower.

A critical thickness of the order of 9 nm for the system $Si_{0.6}Ge_{0.4}/Si(111)$ is obtained from the evaluation of plan-view bright-/dark-field and cross-sectional HRTEM observations. As soon as the layers grow beyond this critical thickness, the nucleation of dislocations takes place. In these specimens with their particular geometry, i.e., the continuous increase of layer thickness towards the step edges, the onset of plastic relaxation can be studied in an ideal way. A plan-view electron micrograph of the stepped layer is shown in Fig. 8. The edges of the steps are aligned in $\langle 1\bar{1}0\rangle$ directions. The layer is mostly defect-free, but in areas close to some step edges, where the thickness has exceeded the critical value, misfit dislocations appear. The misfit dislocation network shows a hexagonal structure, similar to results of LPE growth of SiGe layers on (111) Si substrates published earlier [17, 18]. Here, the isolated straight dislocations are of particular interest because they are characteristic for the onset of plastic relaxation in this system. These dislocations have predominantly step character with $a/2\ \langle 1\bar{1}0\rangle$ Burgers vector and $\langle 11\bar{2}\rangle$ line direction. Stereo micrographs show that these dislocations run along the interface between layer and substrate, bend upwards with a threading segment that ends at the surface of the layer. The nucleation of misfit dislocations takes place at the step edges when the layer exceeds the critical thickness.

Cross-sectional TEM studies just show a more or less arbitrary section of the specimen and do not allow a characterisation of each interesting area in the layer. Such a characterisation is insufficient since the SiGe layer is stepped with a sawtooth profile that is not laterally uniform (cf. Fig. 8). The analysis of rocking profiles in convergent beam electron diffraction patterns taken from plan-view specimens reveals information with high precision from specific areas [15, 19, 20]. When the rocking profile technique is applied, a variety of parameters, which in their entirety are not accessible to another characterisation technique, can be obtained with reasonable accuracy and within a short time. Artefacts due to strain relaxation at the specimen surfaces are of much less significance when plan-view specimens are used.

By using a TEM supplied with an energy filter, a convergent electron probe of 20 nm in diameter was focused onto several positions of a stepped SiGe layer on Si(111) as indicated in Fig. 5. At each position, CBED patterns were recorded with a slow-scan CCD camera. The rocking profiles of certain Bragg lines were extracted from the CCD images

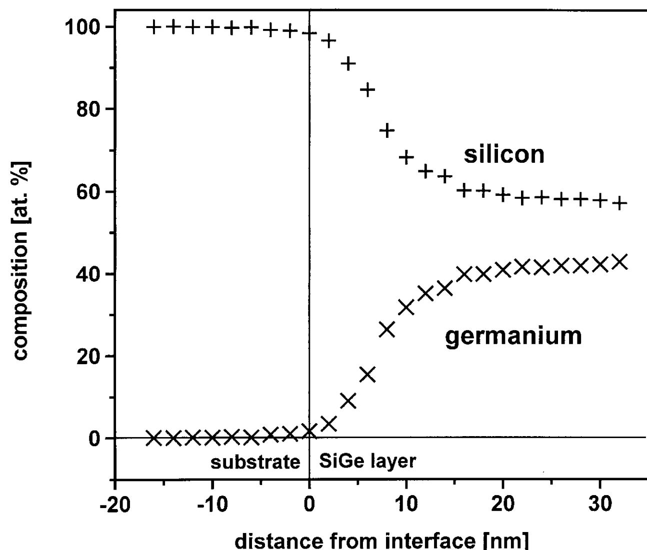

Fig. 7. Composition of a SiGe layer on a (111) Si substrate as a function of the distance from the interface. Measurements by EDX in a dedicated STEM with an electron probe of 1 nm diameter

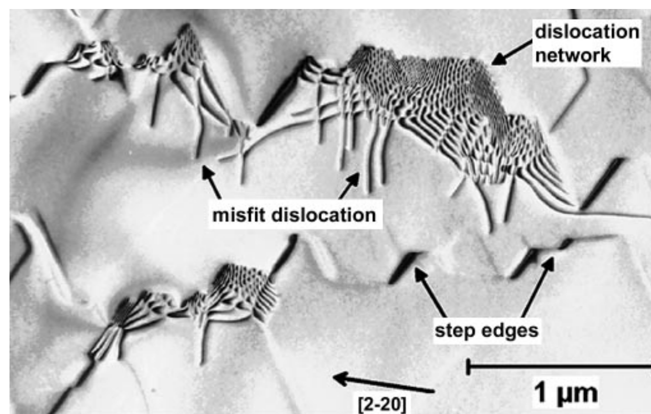

Fig. 8. Plan-view TEM image of a stepped SiGe layer on a (111) Si substrate (cf. Fig. 4). Some step edges are plastically relaxed and show a typical misfit dislocation network. Isolated misfit dislocations (*arrowed*) spread from the relaxed step edges towards the unrelaxed areas of the layer

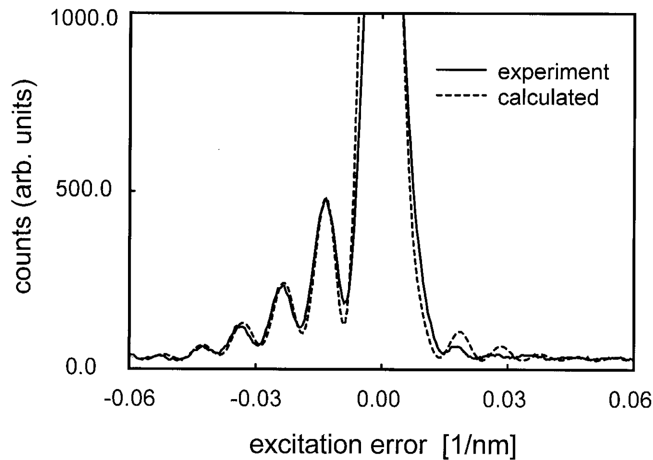

Fig. 9. Rocking profile of a ⟨551⟩ Bragg line in a convergent beam electron diffraction pattern obtained from position 1 (indicated in Fig. 5) on a SiGe layer grown on (111) Si. The calculated profile (*dotted line*) was obtained from a dynamical calculation with fit to the experimental profile. For the calculated profile shown here, a layer thickness of 23.9 nm, a Ge concentration of 13 at. %, and a vertical strain of 0.006 were used

and compared with rocking profiles that were calculated for different parameters of the layers. By varying the thickness, Ge content, and strain in the calculated profiles and fitting to the experimental result, these three parameters could be obtained with good accuracy. Figure 9 shows as an example the rocking profile of a ⟨551⟩ line recorded at position 1 (as indicated in Fig. 5 and Table 1). The pronounced asymmetry of the profile results from the different lattice spacings and strain in the SiGe layer (relative to the unstrained Si substrate where a perfectly symmetrical profile is obtained) [15]. The results of the rocking profile analysis for measurements at 5 positions as shown in Fig. 5 are summarised in Table 1. The Ge content (averaged over the thickness of the layer) increases with increasing layer thickness. This behaviour is due to the increasing Ge concentration with increasing distance from the substrate–layer interface. Because of the low thickness and accordingly low Ge concentration, the results at positions 4 and 5 are rather uncertain. By focusing the electron probe onto step edges where no plastic relaxation has occurred, the critical thickness of the SiGe layers can hence be determined with good accuracy. As an additional parameter, the lattice strain can be deduced from the rocking profiles. At the positions 1–3 in the layer, an averaged vertical strain (normal to the interface) of $\varepsilon = 0.006 \pm 0.003$ is obtained.

3 Discussion

3.1 Driving forces in the growth of strained SiGe *layers*

The thermodynamic driving force β for crystallisation is an important parameter in crystal growth:

$$\beta = \Delta\mu / RT \tag{1}$$

[21, 22], where $\Delta\mu$ is the difference between the chemical potentials of the non-crystalline and the crystalline phase (this corresponds to the supersaturation), R the gas constant and T the temperature. Growth from a solution has the advantage that β can be precisely adjusted around $\beta = 0$ because

Table 2. Surface energies for (111) and (100) faces of Si and Ge [23]. For Ge, the surface energies are given for a relaxed lattice (lattice parameter a_{Ge}) and a strained lattice with the lattice parameter of Si(a_{Si})

		(100)		(111)	
		eV/atom	J/m^2	eV/atom	J/m^2
silicon	a_{Si}	1.97	2.14	1.1	1.38
germanium	a_{Ge}	1.57	1.57	0.98	1.13
	a_{Si}	1.57	1.70	0.98	1.23

$\beta \approx \Delta T / T_{eq}$ [21, 22]. Here ΔT denotes the supercooling of the solution and T_{eq} the temperature where the crystalline phase appears in thermodynamic equilibrium. Thus, unlike vacuum deposition techniques, LPE allows the study of heteroepitaxy uninfluenced by supersaturation.

A further energy term is of particular importance in the crystallisation of thin SiGe layers. The driving force for the initial crystallisation is the difference between the surface free energies of the layer and the substrate. The energies for (111) and (100) faces of Si and Ge are listed in Table 2. The surface free energies are much higher for (100) than for (111) surfaces [23]. As a consequence, (100) surfaces are unstable. The difference between the (100) surface free energies of the substrate and a pseudomorphic $Si_{0.5}Ge_{0.5}$ layer amounts to 0.22 J/m^2 (half of the difference between pure Ge and Si). In the Stranski–Krastanov growth mode, the (100) substrate is first covered by a complied SiGe layer, however, already during the first stage of the growth period, islands with (111) surfaces form. LPE on Si (100) is therefore not practicable for the growth of coherent 2D layers of SiGe on large areas [24]. On the other hand, the islands are free of defects, although the initial growth rate is high. Such growth is difficult to achieve by other techniques.

The difference between the surface free energies of Si and Ge is lower for the (111) than for the (100) surface. The surface free energy of a pseudomorphic $Si_{0.5}Ge_{0.5}$(111) layer is approximately 0.07 J/m^2. Because of the relatively small driving force, the initial growth can take place close to equilibrium. On a (111) Si substrate the SiGe layer is able to grow in a quasi 2D mode ("quasi 2D" because the coherent layer is stepped and not perfectly flat). The transition to 3D island growth occurs after the plastic relaxation of the coherent layer.

Steps on the surface of the substrate determine the morphology of the epitaxial layer; in the LPE process surface steps are unavoidable. The vapour of the solvent has a decisive influence on the step formation during the tempering of the substrate prior to growth, however, this has not yet been investigated in detail until now. The basic growth mechanism in LPE is the lateral propagation of monoatomic steps. When the lateral movement of a step ceases and the next upper layer reaches the step edge, the height of the edge increases by one layer (step bunching). Because such a layer has the possibility to reduce its elastic stress by lateral relaxation at the free step edge, the growth of monatomic layers on a higher level is energetically favoured. Hence, the lateral growth rate can increase with layer thickness as the relaxation at step edges is facilitated. A schematic drawing of this scenario is shown in Fig. 10.

The observed gradient in the Ge concentration can be explained by two effects. (a) The solvent detaches the substrate

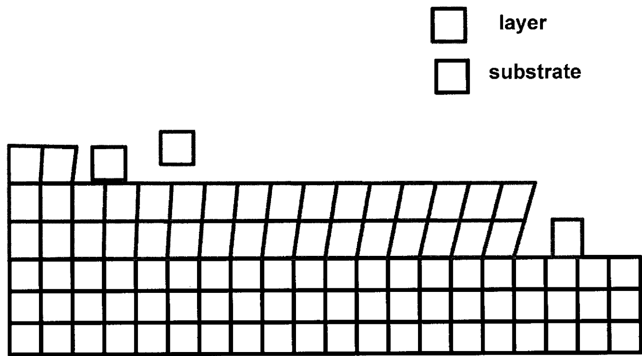

Fig. 10. Schematic drawing of lateral strain relaxation at a step edge of a strained SiGe layer

surface, therefore the Si concentration in the solvent is higher in the initial stage of growth, i.e. the ratio between Si and Ge in the solvent is locally shifted to the Si-rich side. After the deposition of the first monolayers, the substrate is gradually covered by Ge atoms and no further Si dissolves. (b) On a Si substrate, the growth of a Si-rich layer is energetically favoured because of the vanishing elastic energy in the pseudomorphic layer (no strain builds up during growth of pure Si). With increasing height, the Ge concentration increases and long-range stress builds up, but the layer has the possibility to reduce its elastic stress at the free step edge. Thus, the lattice constant of the layer approaches the value of relaxed SiGe and the growth of a Ge-rich layer is favoured.

3.2 *Critical thickness and plastic relaxation*

A model describing the nucleation and propagation of misfit dislocations is schematically shown in Fig. 11. The plastic relaxation of the epitaxial layer starts at the growth front (step edge) where the critical thickness is reached first. The dislocations whose threading segments end at the surface of the layer spread and lengthen along the interface between layer and substrate during further growth. Intersection of misfit dislocations leads to the hexagonal network as observed in the relaxed areas of the layer. Whereas lateral strain relaxation normal to the step edges occurs mainly by the overhanging edges (Fig. 10), the introduction of the isolated misfit dislocations leads to relaxation parallel to the edges (which is the direction of the Burgers vector).

Since we observe that the initial strain relaxation takes place through the nucleation of misfit dislocations with a gliding threading segment, the critical thickness of the layers can be treated in terms of the model of Matthews and Blakeslee (MB) [3, 25]. Two forces act on the dislocation as shown in Fig. 11. The first force, F_ε, originates from the misfit stress

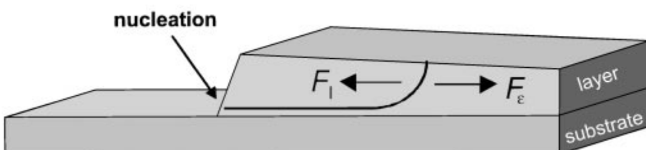

Fig. 11. Driving forces during plastic relaxation of a SiGe layer. The misfit dislocation drawn here (corresponding to those arrowed in Fig. 8) experiences forces from its line tension (F_l) and from the elastic strain (F_ε)

in the film and pulls the free end of the dislocation towards the dislocation-free side (right side in Fig. 11) where strains are still unrelaxed. The second force, F_l, results from the line tension of the dislocation. F_l tends to shorten the misfit dislocation segment and thus pulls the dislocation towards its pinned end at the step edge. The critical thickness of the layer is reached when these two forces are in balance. As soon as F_ε, prevails, the nucleation and propagation of the dislocation is energetically favourable. With increasing thickness of the layer, the misfit segment becomes longer and the dislocation lengthens towards the unrelaxed side.

By considering the balance of these two forces on a threading dislocation, the MB model gives the following relation for the critical thickness h_c of the layer [3]:

$$h_c = \frac{b(1-\nu\cos^2\beta)}{8\pi f_0(1+\nu)\cos\phi} \ln\frac{\alpha h_c}{b} , \tag{2}$$

where b is the magnitude of the Burgers vector, f_0 the misfit, ν the Poisson ratio, β the angle between the Burgers vector and the dislocation line, ϕ the angle between the Burgers vector and the normal on the dislocation line, and α denotes the dislocation core parameter which has the value of 4 for a diamond structure [26]. The experimentally observed misfit dislocations have a Burgers vector $\boldsymbol{b} = a/2\langle 1\bar{1}0\rangle$ and a line direction $\boldsymbol{l} = \langle 11\bar{2}\rangle$; with the angles β and ϕ inserted, (2) reduces to:

$$h_c = \frac{b}{8\pi f_0(1+\nu)} \ln\frac{\alpha h_c}{b} . \tag{3}$$

This relation is shown in Fig. 12 with $\nu = 0.262$ [27] and the experimentally determined value of b. For a SiGe layer with a Ge content of 40% in the upper regions, a critical thickness of 9 nm is obtained. As indicated in Fig. 12, we obtain an effective misfit of 0.6% which is clearly lower than the value of 1.7% which would be expected for a $Si_{0.6}Ge_{0.4}$ layer with uniform Ge distribution.

The discrepancy between the expected critical thickness and the larger experimental value can be explained by the fol-

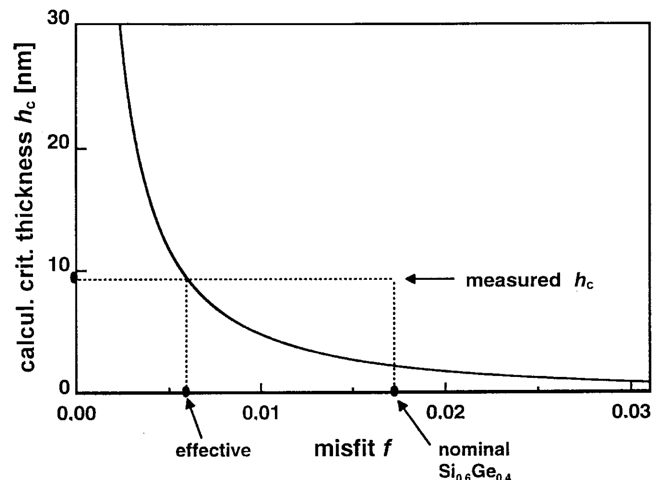

Fig. 12. Critical thickness of a SiGe layer on a (111) Si substrate as a function of the misfit calculated by the modified Matthews–Blakeslee formula (see text). The experimentally derived value is indicated

lowing arguments. (a) The vertical gradient in the Ge concentration reduces the effective misfit. The uniform distribution of the strain over a vertical distance of some 10 nm hinders the nucleation of misfit dislocations, unlike at a sharp interface where the local strain is higher. From the measured concentration profile (Fig. 7) and from the analysis of rocking profiles in CBED patterns, we can estimate a vertically averaged Ge concentration of $\sim 18\%$ for a layer of 9 nm in thickness with a Ge concentration of 40% close to the surface. This would correspond to an effective misfit of 0.75%. (b) The lateral elastic relaxation of the strain is easier at the edges of the stepped layer than in a closed 2D layer. At the edges, a higher critical thickness is therefore possible. The remaining difference of the effective misfits (0.6% obtained from Fig. 12; 0.75% obtained after consideration of the concentration gradient (a)), amounts to 0.15%. We can therefore conclude that an elastic relaxation of 0.15% takes place et the step edges.

These two effects (a) and (b) can be taken into account in the MB formula. We obtain a modified MB relation by replacing the misfit f by the effective misfit f_{eff} which corresponds to the averaged Ge concentration and by adding a thickness h_{el} (a function of f_{eff}, h_{c}, and the area ratio δ of the step side walls and their surface) which considers the elastic relaxation at the step edges:

$$h_{\mathrm{c}} = \frac{b}{8\pi f_{\mathrm{eff}}(1+\nu)} \ln \frac{\alpha h_{\mathrm{c}}}{b} + h_{\mathrm{el}}(f_{\mathrm{eff}}, h_{\mathrm{c}}, \delta) \,. \tag{4}$$

With the semi-empirical term h_{el} we are now able to describe the experimentally determined critical thickness of SiGe layers on (111) Si substrates with the modified MB model.

4 Conclusions

By applying liquid phase epitaxy, SiGe layers were grown on Si substrates with (100) and (111) surfaces. A detailed electron microscopy characterisation was carried out to determine the critical thickness of the layers and to study the onset of plastic relaxation. Unlike in most other epitaxy techniques, growth from solution occurs close to thermal equilibrium. The proximity to equilibrium has the consequence that the energetically unfavourable (100) faces of SiGe layers can not be stabilised and Stranski–Krastanov growth of islands prevails on (100) Si substrates. Other techniques such as MBE are superior in that they can gain from a kinetic stabilisation of the (100) surface. However, near-equilibrium solution growth is favourable when (111) SiGe layers of high quality and large critical thickness have to be achieved. The gradient in the Ge concentration and the lateral relaxation at step edges enable us to grow defect-free layers of high critical thickness and a high Ge concentration in the upper part. This is akin to the growth of graded layers by other techniques.

Acknowledgements. This work was initiated by the late E. Bauser (died 29 September 1996), to whom the authors owe invaluable motivation and an outstanding LPE laboratory. The authors benefited from good collaboration with A. Gutjahr and I. Silier during the LPE experiments. The technical assistance of R. Höschen, W. Olms, A. Weißhardt, M. Kelsch, B. Siegle, J. Thomas, and G. Maier in the electron microscopy work is gratefully acknowledged. Last but not least, the authors wish to thank H.-J. Queisser and A. Seeger for their continuous interest and valuable discussions. This work has been supported by the Volkswagen-Stiftung (grant no. I/71071).

References

1. E. Kasper (Ed.): *Properties of Strained and Relaxed Silicon Germanium* (INSPEC, London 1995)
2. C.A. Ball, H.J. Van der Merwe: In *Dislocations in Solids*, Vol. 6, ed. by F.R.N. Nabarro (North-Holland, Amsterdam 1983) p. 123
3. J.W. Matthews, A.E. Blakeslee: J. Cryst. Growth **27**, 118 (1974)
4. J.W. Matthews: J. Vac. Sci. Technol. **12**, 126 (1975)
5. J.W. Matthews, A.E. Blakeslee, S. Mader: Thin Solid Films **33**, 253 (1976)
6. D.C. Houghton, J.-M. Baribeau, N.C. Rowell: J. Mater. Sci. **6**, 280 (1995)
7. R. People, J.C. Bean: Appl. Phys. Lett. **47**, 322 (1985)
8. E. Bauser,P.O. Hansson, M. Albrecht, H.P. Strunk, A. Gustafsson: Solid State Phenomena **32**-**33**, 385 (1993)
9. P.O. Hansson, F. Ernst, E. Bauser: J. Appl. Phys. **72**, 2083 (1992)
10. P.O. Hansson, E. Bauser, M. Albrecht, H.P. Strunk: Mater. Res. Soc. Symp. Proc. **312**, 53 (1993)
11. T. Füller: PhD thesis, University of Stuttgart 1999
12. E. Bauser: In *Handbook of Crystal Growth*, Vol III, ed. by D.T.J. Hurle (Elsevier, Amsterdam 1994) p. 879
13. W. Kern, D.A. Puotinen: RCA Rev. **6**, 187 (1970)
14. P.O. Hansson, M. Albrecht, W. Dorsch, H.P. Strunk, E. Bauser: Phys. Rev. Lett. **73**, 444 (1994)
15. J. Zipprich, T. Füller, F. Banhart, O.G. Schmidt, K. Eberl: J. Microsc. **194**, 12 (1999)
16. D. Stenkamp, W. Jäger: Appl. Phys. A **57**, 407 (1993)
17. F. Ernst: Philos. Mag. A **68**, 1251 (1993)
18. F. Ernst: Mater. Sci. Eng. A **233**, 126 (1997)
19. D. Cherns, R. Touaita, A.R. Preston, C.J. Rossouw, D.C. Houghton: Philos. Mag. A **64**, 597 (1991)
20. J. Zipprich: PhD thesis, University of Stuttgart 1999
21. H.E. Lundager Madsen: J. Cryst. Growth **85**, 377 (1986)
22. M. Elwenspoek: J. Cryst. Growth **76**, 514 (1986)
23. J.L. Mercer Jr., M.Y. Chou: Phys. Rev. B **48**, 5374 (1993)
24. P.O. Hansson, M. Albrecht, H.P. Strunk, E. Bauser, J.H. Werner: Thin Solid Films **216**, 199 (1992)
25. R. Hull, J.C. Bean: Crit. Rev. Solid State Mater. Sci. **17**, 507 (1992)
26. J.P. Hirth, J. Lothe: *Theory of Dislocations*, 2nd. edn. (Wiley, New York 1982)
27. W.A. Brantley: J. Appl. Phys. **44**, 534 (1973)